Characterization of an Optimized Light Source and Comparison to Pulsed Dye Laser for Superficial and Deep Vessel Clearance

Robert A. Weiss, MD,[1] E. Victor Ross, MD,[2] Emil A. Tanghetti, MD,[3] David B. Vasily, MD,[4] James J. Childs, PhD,[5*] Mikhail Z. Smirnov, PhD,[5] and Gregory B. Altshuler, PhD[5]

[1]*Maryland Laser Skin and Vein Institute, Hunt Valley, Maryland 21030*
[2]*Scripps Clinic Carmel Valley, San Diego, California 92130*
[3]*Center for Dermatology and Laser Surgery, Sacramento, California 95819*
[4]*Aesthetica Cosmetic and Laser Surgery Center, Bethlehem, Pennsylvania 18018*
[5]*Palomar Medical Technologies, Burlington, Massachusetts 01803*

Background and Objective: An arc lamp-based device providing optimized spectrum and pulse shape was characterized and compared with two pulsed dye laser (PDL) systems using a vascular phantom. Safety and effectiveness for facial telangiectasia are presented in clinical case studies.

Study Design/Materials and Methods: An optimized pulsed light source's (OPL) spectral and power output were characterized and compared with two 595 nm PDL devices. Purpuric threshold fluences were determined for the OPL and PDLs on Fitzpatrick type II normal skin. A vascular phantom comprising blood-filled quartz capillaries beneath porcine skin was treated by the devices at their respective purpuric threshold fluences for 3 ms pulse widths, while vessel temperatures were monitored with an infrared (IR) camera. Patients with Fitzpatrick skin types II–III received a split-face treatment with the OPL and a 595 nm PDL.

Results: The OPL provided a dual-band output spectrum from 500 to 670 nm and 850–1,200 nm, pulse widths from 3 to 100 ms, and fluences to 80 J/cm^2. The smooth output power measured during all pulse widths provides unambiguous vessel size selectivity. Percent energy in the near infra-red increased with decreasing output power from 45% to 60% and contributed 15–26% to heating of deep vessels, respectively. At purpuric threshold fluences the ratio of OPL to PDL vessel temperature rise was 1.7–2.8. OPL treatments of facial telangiectasia were well-tolerated by patients demonstrating significant improvements comparable to PDL with no downtime.

Conclusions: Intense pulsed light (IPL) and PDL output pulse and spectral profiles are important for selective treatment of vessels in vascular lesions. The OPL's margin between purpuric threshold fluence and treatment fluence for deeper, larger vessels was greater than the corresponding margin with PDLs. The results warrant further comparison studies with IPLs and other PDLs. Lasers Surg. Med. 43:92–98, 2011.

Key words: arc lamps; intense pulsed light; photothermolysis; purpura; purpuric threshold fluence; telangiectasia; vascular lesions; vascular phantom

INTRODUCTION

It has long been established that vascular lesions of the skin, including port wine stains, telangiectasia, and rosacea respond to treatment with lasers such as the pulsed dye or frequency-doubled Nd:YAG lasers [1–4]. Reports have also shown that treatment with traditional broad-spectrum intense pulsed light (IPL) devices provide clearance of vascular lesions, though for some indications to a lesser degree than with lasers [5,6]. Recently, a direct comparison study has demonstrated similar results for clearance of Port Wine Stains, both resistant and previously untreated, with a long-pulse pulsed dye laser (PDL) and an IPL [7].

In this work, an optimized pulsed light source (OPL) is characterized and evaluated clinically and in an ex vivo vascular phantom. The OPL is an arc lamp with spectral, pulse shape and fluence matching for vascular targets. An optimal device will thermally affect only the target blood vessels with no injury to surrounding tissue, other blood vessels, or to the melanin-containing dermal/epidermal junction. In practice, this is accomplished using principles of the extended theory of selective photothermolysis [8] by

Disclosures: James Childs, Palomar Medical Technologies, Inc., Employee; Mikhail Smirnov, Palomar Medical Technologies, Inc., Employee; Gregory Altshuler, Palomar Medical Technologies, Inc., Employee; Robert Weiss, Maryland Laser Skin and Vein Institute, Equipment and Research Consultant for PMTI; E. Victor Ross, Scripps Health, Equipment and Research Consultant for PMTI; David Vasily, Aesthetica Cosmetic and Laser Surgery Center, Equipment and Research Consultant for PMTI; Emil Tanghetti, Center for Dermatology and Laser Surgery, Equipment from PMTI.

*Corresponding to: Dr. James J. Childs, PhD, Palomar Medical Technologies, 15 Network Drive, Burlington, MA 01803.
E-mail: jchilds@palomarmedical.com

Accepted 7 December 2010
Published online 25 February 2011 in Wiley Online Library (wileyonlinelibrary.com).
DOI 10.1002/lsm.21032

© 2011 Wiley-Liss, Inc.

targeting the chromophore hemoglobin within erythrocytes. The light is absorbed by hemoglobin and converted to heat that then conducts or convects to the vessel walls and, if sufficient, coagulates and clears the vessel. The range of target vessel sizes and depths found in vascular lesions requires a range of energies, pulse widths, and wavelengths dictated by the principles of selective photothermolysis and tissue optics. The short wavelengths such as 577, 585, or 595 nm used in PDLs are highly absorbed by hemoglobin which decreases the laser power requirements but these wavelengths also have limited penetration depth [9,10]. For treatment of larger vessels with longer pulse widths, PDLs and most IPLs emit a train of shorter pulses due to the high lasing thresholds and the use of free-discharge, capacitor power supplies, respectively [11–13]. In addition to increasing the cooling demands for the epidermis, a pulse train cannot treat larger vessels without also affecting smaller vessels. Consequently, the purpuric threshold fluence is lowered.

MATERIALS AND METHODS

Device Description and Characterization

The OPL has a Xenon arc lamp filtered to provide a dual-band spectral output in the 500–670 nm range and in the 870–1,200 nm range (MaxG™; Palomar Medical Technologies, Inc., Burlington, MA). The handpiece was driven by a power-source supply capable of providing smooth output power during pulse widths from 3 to 100 ms with fluences from 5 to 85 J/cm^2 (Icon™; Palomar Medical Technologies, Inc.). The treatment area is defined by a 10 mm $\times$ 15 mm sapphire optical window whose temperature can be maintained at 5 or 15°C for contact skin cooling. The PDL systems used in this study included the VBeam™ and the Perfecta™ (Candela Corp, Wayland, MA) as well as the V-Star® (Cynosure, Westford, MA).

The OPL output spectrum was measured with three spectrometers covering wavelength ranges 300–1,040, 800–1,100, and 900–2,100 nm (RPS900-R, International Light Technologies, Peabody, MA, NIR512 and NIR256-2.1, Ocean Optics, Dunedin, FL, respectively). All spectrometers are calibrated for irradiance with an LS-1 Cal lamp (ser #LSC1406; Ocean Optics, Dunedin, FL) operating at a color temperature of approximately 3,100 K and its associated calibration data as provided by the manufacturer. The OPL spectrum was also digitized by energy measurements with two Schott glass long-pass filters at 400 and 715 nm wavelengths. Energy measurements were performed over a range of pulse widths and fluence settings with a broad-band Ophir energy meter and with one of the filters in optical contact with the sapphire output window. For a given device setting, an energy measurement with the 715 nm wavelength filter was subtracted from the measurement with the 400 nm wavelength filter to provide energy in the green (visible) passband. These measurements then provided the percentage of total energy in the visible and near infra-red spectral (NIR) regions to measure power-dependent spectral shifts. Output pulse profiles of the OPL device were measured with a silicon photodiode placed in front of the output sapphire window with neutral density filtration to avoid detector saturation. The photodiode output was recorded on an oscilloscope (TDS 2022B, Tektronix, Beaverton, OR) with 200 MHz bandwidth.

Vascular Phantom

A vascular phantom was constructed to measure the temperature rise in blood vessels following exposure to purpuric threshold fluences from the OPL and PDL devices. Purpuric threshold fluences were determined by administering test spots to the volar forearm or back of volunteer subjects with Fitzpatrick Skin type II skin. Pulse widths were 3, 5, and 10 ms for the OPL device and 3, 6, and 10 ms for the PDL devices. For each pulse width, the fluence was incrementally increased until purpura was observed over 80% of the area 10 minutes after treatment. Cooling was provided by adjusting the temperature of the sapphire window to 15°C for the OPL and via the dynamic cooling device (DCD®; Candela Corp., Wayland, MA.) for the PDL. Light pressure was maintained throughout OPL treatment to avoid vessel compression.

The phantom blood vessels consisted of 100, 200, and 500 μm diameter quartz capillaries filled with 15 g/dl hemoglobin concentration (Bovine hemoglobin in deionized water, Cat. #H3760-100; SIGMA, Ronkonkoma, NY). Hemoglobin spectra were obtained with a spectrophotometer (Lambda 950; Perkin Elmer, Waltham, MA). Yucatan white porcine skin was shaved, cleaned, and the fat layer removed to leave approximately 1–1.5 mm of dermis with the epidermis and stratum corneum intact. The skin was placed over the capillaries with skin surface side up. A mirror beneath the skin and capillary phantom allowed the capillaries to be imaged with a calibrated FLIR 4000 infrared (IR) camera (FLIR Systems, Billerica, MA) from below. The top half of the capillaries were in contact with the dermis, while their bottom surfaces were exposed to air. The IR camera viewed the lower regions of the capillaries with minimal intervening water between the camera and exposed vessel. The handpiece was then placed on the skin surface above the capillaries and the IR camera recorded the phantom vessel temperatures during and after the pulse. The sequence of test parameters was repeated in reverse order to monitor systematic drifts.

To experimentally assess the contribution of the NIR portion of the OPL output spectrum to deep vessel heating, the handpiece was modified by attaching one of two long-pass filters to the output face of the OPL sapphire window. A 715 nm long-pass filter allowed only the NIR portion of the output spectrum and a 400 nm long-pass filter passed the entire spectrum of the OPL. The interface conditions of the sapphire window and skin of the phantom were the same for both long-pass filters.

Computer Simulations

A Monte Carlo model was used to simulate photon propagation in Fitzpatrick type II skin. Tissue thermal

and optical properties were taken from the literature. The combined optical and thermal problem was solved using a finite elements technique in two-dimensional geometry. A full description of the model has been given elsewhere [14]. Heat production curves for blood vessels were produced by weighting the hemoglobin absorption coefficients at each wavelength with the ratio of the local fluence at the depth of the blood vessel to the local fluence at the skin surface. Heat production curves therefore account for the wavelength-dependent attenuation of light in the tissue to provide the blood vessel heating capability.

Clinical Studies

To evaluate the clinical efficacy of the OPL for the treatment of facial telangiectasia, subjects received a single split-face treatment with the OPL and 595 nm PDL (V-Star®; Cynosure, Westford, MA). Settings for all devices were optimized based on the size of the vessels and severity and extent of facial telangiectasia. OPL settings for smaller vessels were 36 J/cm^2 and 10 ms pulse width and larger vessels were treated with 60 J/cm^2 and 100 ms pulse width. PDL settings ranged from 8.1 to 8.5 J/cm^2 and 10 ms pulse widths using the 10 mm spot. Larger vessels were treated with the 7 mm spot size at 14 J/cm^2 and 40 ms pulse width.

RESULTS

Device Characterization: Pulsed Power Profile

Output power pulse shapes from the OPL and the PDL devices are compared in Figure 1 for 3 ms 27 J/cm^2, 10 ms 36 J/cm^2, and 6 ms 7.5 J/cm^2, respectively. Note that the OPL output power was uniform throughout the pulse width, whereas the PDL output power consisted of a train of four shorter (100 μs) pulses of high peak-power spikes during the pulse width [11]. Other OPL pulse widths exhibited similar smooth-pulse structure. The OPL peak intensity was the same as the average intensity during the 10 ms pulse width (3.6 kW/cm^2), whereas the peak intensity of each micro-pulse was much higher (18.75 kW/cm^2) than the average intensity (1.25 kW/cm^2) during the PDL's 6 ms pulse width. Note that intensity is a measure of output power and equals the total fluence in J/cm^2 divided by pulse width in milliseconds. The units for intensity are kilowatts per unit area (kW/cm^2).

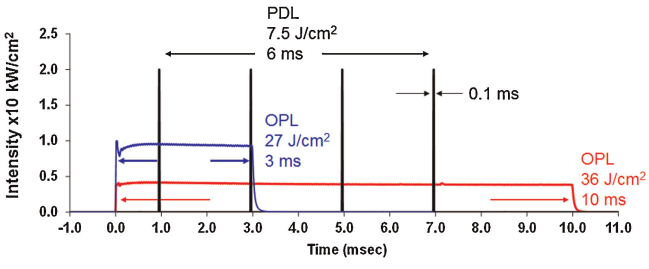

Fig. 1. Typical output power traces for OPL are shown for 3 ms (blue) and 10 ms (red) pulse widths. The PDL output power trace (black) corresponds to a 6 ms pulse width and consists of 4 100 μs pulses within the 6 ms pulse width.

Device Characterization: Spectrum and Spectral Shift

In contrast to the single wavelength of a PDL device, the OPL output consists of a dual-band spectrum depicted by the green curve in Figure 2 and superimposed on the heat production curves of venous blood and methemoglobin (MetHb) within vessels at a 500 μm depth. The spectrum from 300 to 2,000 nm is obtained by combining measurements with three different spectrometers after dark count subtraction and scaling to match the absorption levels in the overlap regions. The measurements provide the average spectral output for the entire pulse. Finally, a digital smoothing filter with 35 nm band-width is applied. The first band from 500 to 670 nm overlaps the Q-bands of hemoglobin, whereas the second band emitting from 850 nm on overlaps the NIR absorption bands of hemoglobin.

Figure 3 displays percentage of total energy in the visible (in green, 400–670 nm) and NIR regions (in red, 715–1,500 nm) of the OPL device's spectrum for selected fluence and pulse width settings. As output power is decreased by changing parameters from 3 ms 26 J/cm^2 to

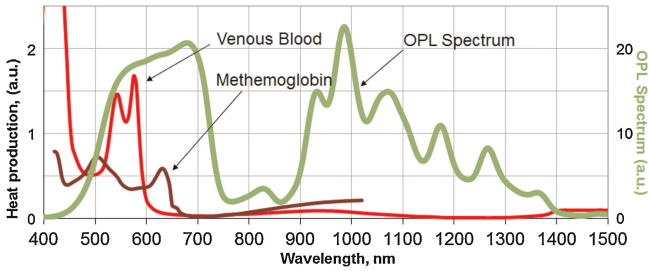

Fig. 2. Heat production curves for venous blood (red curve) and MetHb blood (brown curve) within a 300 μm diameter blood vessel located 0.5 mm below the surface of skin type II are superimposed on the OPL output spectrum taken with settings 46 J/cm^2 and 20 ms pulse width (green curve).

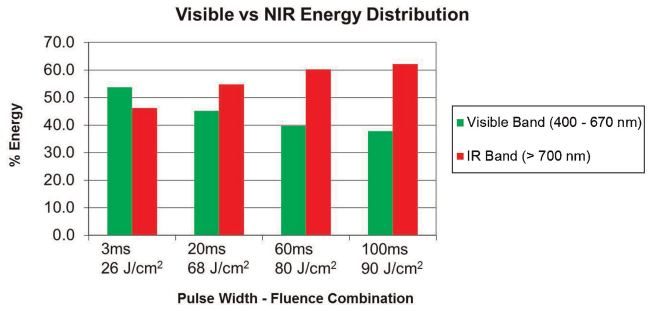

Fig. 3. Filtered output measurements provide the visible (green bars) and NIR (red bars) energy distribution of the OPL at four power settings, 3 ms 26 J/cm^2, 20 ms 68 J/cm^2, 60 ms 80 J/cm^2, and 100 ms 90 J/cm^2.

100 ms 90 J/cm^2, the visible energy decreases by 30% with commensurate increase in the near-IR energy.

Theoretical Considerations and Computer Simulations

Monte Carlo simulations illustrate the advantages of increased NIR with longer pulse widths of the OPL for deeper vessels of 300 μm diameter located 300, 600, and 900 μm below the surface of type II skin (Fig. 4). The color bar describes the fraction of coagulation induced by a single pulse of a PDL (595 nm, 6 ms, 7.5 J/cm^2) and by the OPL handpiece (10 ms, 36 J/cm^2). The deeper vessels are uniformly coagulated (red region) with the OPL, whereas the PDL coagulates only the upper portion of the vessels that can cause incomplete closure.

Vascular Phantom

The volar forearm (1 day post-treatment, Fig. 5a) and back (10 minutes post-treatment, Fig. 5b) of a subject was treated at 3–10 ms pulse widths with a matrix of increasing fluence until purpura was observed. Treatment parameters are displayed in boxes surrounding the corresponding treatment area. For the volar forearm, purpuric thresholds were observed at fluences of 7.5 J/cm^2 versus 26 J/cm^2 for PDL and OPL, respectively, at 3 ms pulse widths. For the back, purpuric thresholds were observed at 8 J/cm^2 versus 38 J/cm^2 for PDL and OPL, respectively. Table 1 summarizes the fluences, the phantom vessel temperature rise, and ratio of the temperature rise of OPL to PDL at the devices' respective purpuric thresholds.

To determine the contribution of the NIR band to heating of 100 μm phantom vessels temperature traces were measured with the OPL output filtered by each of the long-pass filters. Based on the maximum temperatures, approximately 15% of the vessel heating arises from the NIR portion of the device's output spectrum. The OPL device parameters were 36 J/cm^2 and 3 ms pulse width corresponding to a power intensity of 12 kW/cm^2. At this setting, the NIR portion of the total output energy is approximately 43%.

Clinical Case Studies

Figure 6 shows a patient with bilateral telangiectasia across the cheeks and nose. The efficacy of the OPL and PDL (V-Star®) were compared after each side received only one treatment. A total of two passes were delivered to the left side of the patient's face with OPL settings 36 J/cm^2 and 10 ms for smaller vessels and 60 J/cm^2 and 100 ms for larger vessels. The patient's right side of the face was treated with two PDL passes using a 10 mm spot and pulse stacking at 8.3 J/cm^2 and 10 ms for smaller vessels. Both sides displayed significant reductions in erythema and vessel appearance 2 months after treatment.

Another direct comparison between the OPL and a PDL was performed on the patient shown in Figure 7. The left side was treated with two passes of the OPL as with the previous patient and the right side received two passes with the PDL (first pass at 8.2 J/cm^2 and 10 ms with pulse stacking). This patient also exhibited bilateral reductions in vasculature and facial erythema after one treatment.

DISCUSSION

Purpura may provide evidence for the effectiveness of a device on more superficial, small vessels of the dermal plexus whereas the vessel phantom provides a measure of the effectiveness on deeper, larger vessels. The photo in Figure 5b shows that both devices can induce purpura on the back at 3 ms pulse widths whereas only the OPL delivered sufficient fluence to induce purpura at the next available pulse width. The results summarized in Table 1 demonstrate that at purpuric threshold fluences the OPL heats larger vessels more effectively than the PDL. This suggests that the OPL can treat vessels with a greater margin below purpuric threshold. Note that no significance is attributed to the comparison of purpuric fluences at different anatomic sites treated at different times.

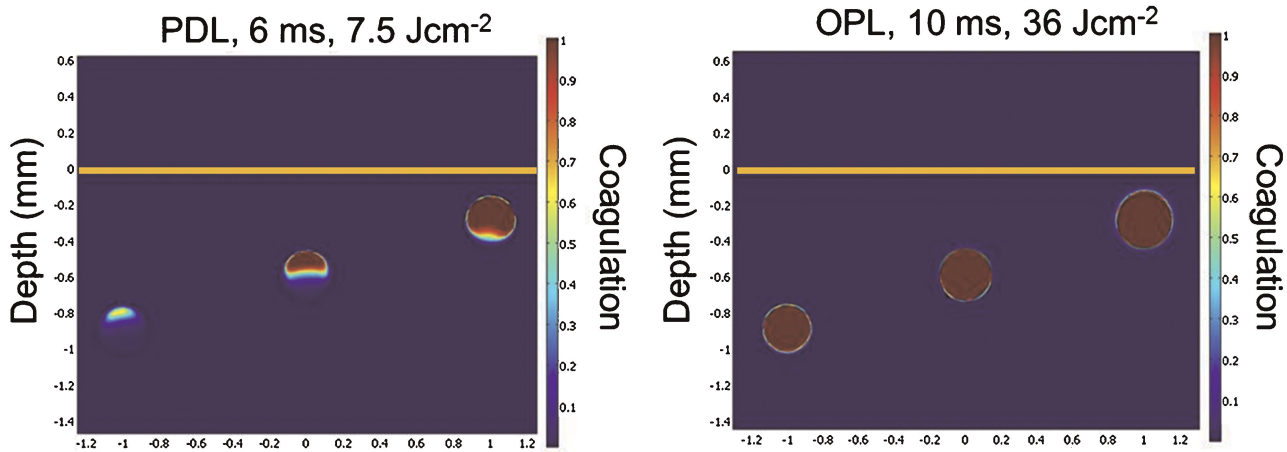

Fig. 4. Full coagulation is depicted by the red region in 300 μm diameter vessels at depths 300, 600, and 900 μm in skin type II. Operating wavelength of the PDL system is 595 nm.

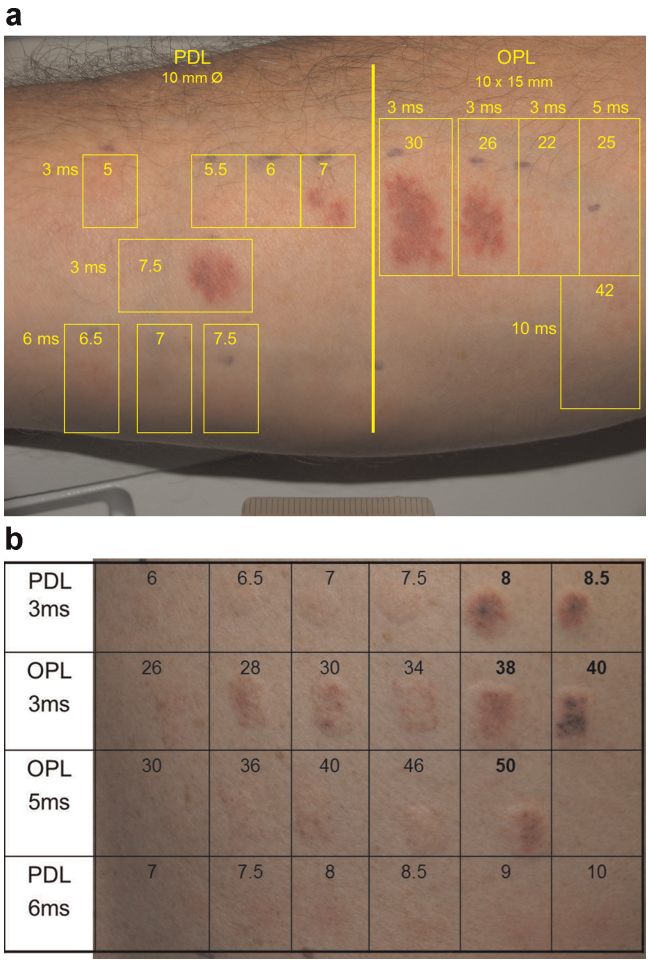

Fig. 5. **a**: Test spots for purpura on the volar forearm of a subject with Fitzpatrick type II skin. Fluences (J/cm^2) are provided within the respective treatment sites. Purpuric thresholds occurred at 7.5 J/cm^2 for PDL and at 26 J/cm^2 for OPL. **b**: Matrix of test spots for purpura on the back of a subject with type II skin. Fluences (J/cm^2) are provided within the respective treatment sites. Purpuric thresholds occurred at fluences of 8 J/cm^2 for PDL and 38 J/cm^2 for OPL.

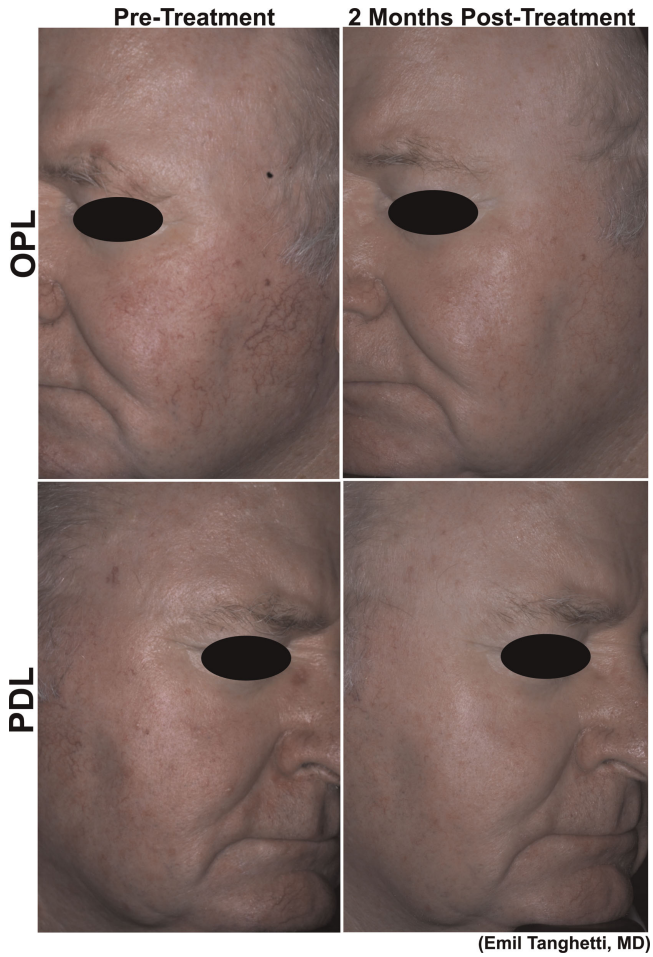

Fig. 6. Patient with Fitzpatrick skin type II received one split-face treatment. Right side received two passes with the OPL at 36 J/cm^2 at 10 ms for smaller vessels and 60 J/cm^2 at 100 ms for larger vessels. Left side received two passes with a PDL using pulse stacking with a 10 mm spot size at 8.3 J/cm^2 and 10 ms and a 7 mm spot at 14 J/cm^2 and 40 ms for larger vessels. Vessel clearance and/or reduction was achieved on both sides at 2 months following treatment.

One contributing factor to the phantom results can be understood by comparing the spectral output of the two devices. PDL devices that utilize a single, short wavelength have limited penetration through larger vessels or to vessels lying deeper in the dermis [9,10]. The short, high-absorption wavelengths are effective on smaller, more superficial vessels, but can cause non-uniform heating of the larger blood vessels' walls and incomplete

TABLE 1. Phantom 100 μm Vessel Temperature Rise at Purpuric Threshold Fluences for 3 ms Pulse Widths With OPL and PDL Devices

Site (device)	Pulse width (ms)	Purpuric fluence threshold (J/cm^2)	Phantom vessel temperature rise (°C)	Phantom vessel temperature rise ratio (OPL/PDL)
Back (Perfecta^{TM} PDL)	3	8	6	2.5
Back (OPL)	3	38	15	
Volar Forearm (VBeam^{TM} PDL)	3	7.5	18	1.7
Volar Forearm (OPL)	3	26	31	

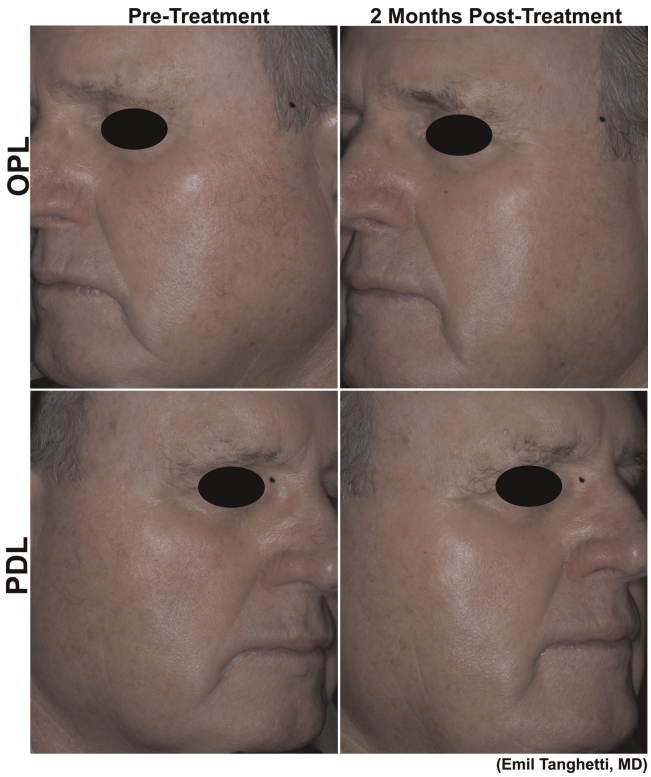

Fig. 7. Patient with Fitzpatrick skin type III received one split-face treatment. Right side was treated with a first pass of the OPL at 36 J/cm^2 and 10 ms and a second pass at 60 J/cm^2 and 100 ms. Left side was treated with two passes of the PDL with pulse stacking at 8.2 J/cm^2 and 10 ms and 14 J/cm^2 and 40 ms for larger vessels. Bilateral vessel reduction was observed at 2 months following treatment.

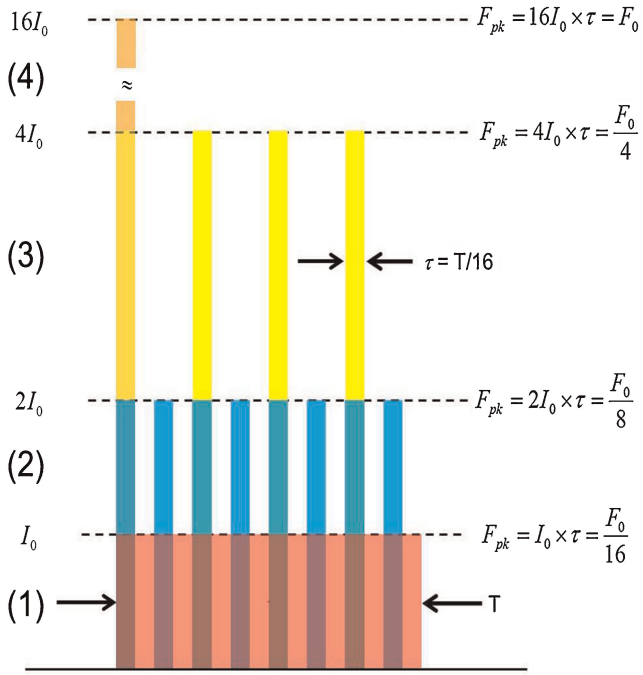

Fig. 8. Four pulse structures that provide a fluence F_0 in a pulse width T.

closure as seen in the simulation results (Fig. 4). The OPL provides appreciable heating of vessels via the NIR portion of the spectrum that has better penetration into the skin.

Another contributing factor to the results can be seen in the analysis of the effect of pulse structure on blood vessels. The fluence, F_0, needed to coagulate a vessel of size corresponding to a thermal relaxation time (TRT) T depends on vessel size and can be delivered in many different ways, four of which are overlaid onto each other in Figure 8. The red structure (1) corresponds to that of the OPL (Fig. 1) and delivers constant intensity (power/area), $I(t) = I_0$, over the pulse width T matching the target vessel's TRT. The blue/blue-green pulse structure (2) consists of 8 micro-pulses each with intensity $2I_0$ and pulse width τ. The yellow (3) and orange (4) pulse structures consist of 4 and 1 micro-pulses each with intensity $4I_0$ and $16I_0$, respectively. Note that all four structures deliver a total fluence F_0 in a time T.

Consider the effect of these pulse structures on a smaller vessel with diameter 4 times less than the target vessel's diameter and TRT = T/16. The vessel temperature at time $\tau = T/16$ is proportional to the fluence, F_{pk}, delivered to the vessel at the end of a micro-pulse. The values are calculated on the right side of the figure for each of the pulse structures. Structure (4) with one micro-pulse within the train delivers the greatest fluence to the vessel within the TRT therefore increasing the chance of coagulation. The minimum fluence delivered to the smaller vessels is realized with the pulse structure (1). For the remainder of a pulse train, the peak temperature reached by successive micro-pulses will increase from pulse to pulse by an amount dependent on the time between micro-pulses. For example, the cooling that occurs between micro-pulses is less in (2) than in (3) so that successive micro-pulses in (2) will be treating a warmer vessel. For a train of pulse width $T = 16\tau$ consisting of a single micro-pulse the maximum temperature will be proportional to $F_{\mathrm{pk}} = F_0$ and is $T_{\max} = T_0$. The temperature at the end of the first micro-pulse of pulse trains (2) and (3) is $T_0/4$ and $T_0/8$, respectively. The maximum temperature reached during these pulse trains can be approximated with a correction factor for the temperature after the first micro-pulse given by $\frac{1}{1-e^{-N}}$ where N is the number of τ pulse widths within the time between micro-pulses. This approximation neglects cooling during the micro-pulses and therefore over-estimates the temperature. The over-estimate increases with the number of micro-pulses. For pulse trains (2) and (3) $N = 1$ and 3, respectively. The ratio of the maximum small-vessel temperature rise caused by a pulse train to that caused by the train with single micro-pulse is summarized in Table 2. Note that pulse structure (1) may be viewed as a train of contiguous pulses each of width τ with no inter-

TABLE 2. Ratio of Small-Vessel Temperature Rise at the End of a Train of Micro-Pulses to the Temperature Rise Caused by a Train With One Micro-Pulse

# Micro-pulses in pulse train	1	4	8
Ratio of small vessel temperature	1	0.26	0.2

The overall fluence and pulse width is the same for all pulse trains.

pulse spacing and will provide the lowest maximum temperature of these vessels.

Finally, a third characteristic of the OPL that contributes to the phantom and clinical results may be described by the measurements and observations shown in Figure 3. As the output intensity of the OPL is decreased to target larger vessels, for example by increasing pulse width by a factor greater than the increase in fluence, a spectral shift arises naturally from decreased temperature in the lamp gas discharge. Lowering the gas discharge temperature shifts energy from the visible portion of the spectrum into the NIR (see also Ref. 12). Considering the treatment parameters of Figure 6, for example, the output intensity is decreased from 3.6 kW/cm^2 for the first pass to 0.6 kW/cm^2 for the second pass (36 J/cm^2 and 10 ms pulse width to 60 J/cm^2 and 100 ms pulse width, respectively) with an approximate 20% increase in NIR energy. The longer wavelengths of light penetrate better into the skin and through larger vessels than the shorter wavelengths because the tissue scatter and absorption is less. The phantom study results together with the device characteristics displayed in Figure 3 imply that up to approximately 30% of deep vessel heating arises from the NIR portion of the OPL's spectrum. Note that the pulse structure also affects the spectral shift. In the case of a non-uniform pulse profile such as a train of shorter pulses, the higher peak-power emitted during the short pulses create momentary higher temperatures within the discharge gas of the lamp that shift the spectrum to the shorter wavelengths and partially neutralize the shift to longer wavelengths occurring over the entire pulse train. A uniform square-pulse profile of the OPL shown in Figure 1 maximizes this spectral shift.

CONCLUSION

The basis for optimal treatment of vascular lesions has been discussed and an OPL source with features fundamentally distinct from PDL and intense pulsed-light devices has been characterized and evaluated in a vascular phantom setup and in clinical case studies. Blood vessel selectivity can be accomplished with optimum fluence, spectral, and pulse width matching. The inherent diversity of vessel sizes and depths within vascular lesions requires a device providing a well-defined range of wavelengths, pulse widths, and fluences. The features of the OPL and power supply that distinguish it from PDLs and IPLs include a bimodal spectral distribution matching the hemoglobin absorption spectra, a smooth output power pulse profile, and maximal spectral shift with changes in device output power. The OPL provides a wider margin for purpura-free treatment of larger vessels than the PDLs. Effectiveness of the device for treatment of smaller, more superficial vessels is also suggested by the ability to cause purpura. More comparative studies of this device with PDLs and IPLs would be helpful to further explore these ideas.

REFERENCES

1. Garden JM, Tan OT, Kerschmann R, Boll J, Furumoto H, Anderson RR, Parrish JA. Effect of dye laser pulse duration on selective cutaneous vascular injury. J Invest Dermatol 1986;87(5):653–657.
2. Garden JM, Polla LL, Tan OT. The treatment of port-wine stains by the pulsed dye laser. Analysis of pulse duration and long-term therapy. Arch Dermatol 1988;124(6):889–896.
3. Bernstein EF, Lee J, Lowery J, Brown DB, Geronemus R, Lask G, Hsia J. Treatment of spider veins with the 595 nm pulsed-dye laser. J Am Acad Dermatol 1998;39 (5 Pt 1):746–750.
4. Yang MU, Yaroslavsky AN, Farinelli WA, Flotte TJ, Rius-Diaz F, Tsao SS, Anderson RR. Long-pulsed neodymium:yttrium-aluminum-garnet laser treatment for port-wine stains. J Am Acad Dermatol 2005;52 (3 Pt 1):480–490.
5. Faurschou A, Togsverd-Bo K, Zachariae C, Haedersdal M. Pulsed dye laser vs. intense pulsed light for port-wine stains: A randomized side-by-side trial with blinded response evaluation. Br J Dermatol 2009;160(2):359–364.
6. Jorgensen GF, Hedelund L, Haedersdal M. Long-pulsed dye laser versus intense pulsed light for photodamaged skin: A randomized split-face trial with blinded response evaluation. Lasers Surg Med 2008;40(5):293–299.
7. Babilas P, Schreml S, Eames T, Hohenleutner U, Szeimies RM, Landthaler M. Split-face comparison of intense pulsed light with short- and long-pulsed dye lasers for the treatment of port-wine stains. Lasers Surg Med 42(8):720–727.
8. Altshuler GB, Anderson RR, Manstein D, Zenzie HH, Smirnov MZ. Extended theory of selective photothermolysis. Lasers Surg Med 2001;29(5):416–432.
9. Fiskerstrand EJ, Svaasand LO, Kopstad G, Ryggen K, Aase S. Photothermally induced vessel-wall necrosis after pulsed dye laser treatment: Lack of response in port-wine stains with small sized or deeply located vessels. J Invest Dermatol 1996;107(5):671–675.
10. Woo SH, Ahn HH, Kim SN, Kye YC. Treatment of vascular skin lesions with the variable-pulse 595 nm pulsed dye laser. Dermatol Surg 2006;32(1):41–48.
11. Kimel S, Svaasand LO, Cao D, Hammer-Wilson MJ, Nelson JS. Vascular response to laser photothermolysis as a function of pulse duration, vessel type, and diameter: Implications for port wine stain laser therapy. Lasers Surg Med 2002;30(2):160–169.
12. Eadie E, Miller P, Goodman T, Moseley H. Time-resolved measurement shows a spectral distribution shift in an intense pulsed light system. Lasers Med Sci 2009;24(1): 35–43.
13. Town G, Ash C, Eadie E, Moseley H. Measuring key parameters of intense pulsed light (IPL) devices. J Cosmet Laser Ther 2007;9(3):148–160.
14. Ross EV, Smirnov M, Pankratov M, Altshuler G. Intense pulsed light and laser treatment of facial telangiectasias and dyspigmentation: Some theoretical and practical comparisons. Dermatol Surg 2005;31 (9 Pt 2):1188–1198.